Hindawi
Advances in Materials Science and Engineering
Volume 2020, Article ID 2978128, 12 pages
https://doi.org/10.1155/2020/2978128

Research Article

The Use of Agricultural Waste Straw to Enhance Loess Shearing Behaviour: An Experimental Investigation

Lin Wang[1,2], **Wen-Chieh Cheng**[1,2] and **Zhong-Fei Xue**[1,2]

[1]*School of Civil Engineering, Xi'an University of Architecture and Technology, Xi'an 710055, China*
[2]*Shaanxi Key Laboratory of Geotechnical and Underground Space Engineering (XAUAT), Xi'an 710055, China*

Correspondence should be addressed to Wen-Chieh Cheng; w-c.cheng@xauat.edu.cn

Received 9 June 2020; Revised 28 July 2020; Accepted 12 August 2020; Published 14 October 2020

Academic Editor: Tomasz Trzepieciński

Strata erosion in northwest China has become an engineering concern as a result of overdevelopment of land. This issue is more distinct for loess soil than other soils since it is characterised by metastable microstructure, high porosity, and water sensitivity. This study explores the potential for the use of agricultural waste straw as a recycled reinforcement material to form the enhanced shearing behaviour towards preventing instability of the loess body. The stress-strain relation and the pore pressure behaviour of Lantian loess and reinforced Lantian loess were studied using the conventional triaxial compression (CTC) stress path for three different confining pressures. Comparison with Jingyang loess and Delhi silt of similar relative fraction of silt to clay, sheared under the reduced triaxial compression (RTC) stress path and the reduced triaxial extension (RTE) stress paths, respectively, was conducted, with emphasis on strength uniqueness and critical state behaviour, to shed light on the effect of waste straw inclusions. The results indicate that the stress path in undrained compression and extension tests had a pronounced effect on the stress-strain relation of the studied soils. Insertion of the waste straw in Lantian loess restrained the development of volumetric deformation, producing higher pore pressures than Lantian loess (unreinforced). This study explores an exciting potential for the use of agricultural waste straw to prevent instability of the loess body in hilly-gullied regions of northwest China when subjected to quick surface thick fills.

1. Introduction

The Chinese Loess Plateau, located in northwest China, is prone to strata erosion due to the overdevelopment of land, which has caused an ecoenvironmental crisis, e.g., shortage risk of water resources, and also affected the livelihood of local farmers over the past two decades despite the application of many countermeasures available [1–10]. Yan'an New District, which has been built along with the Western China Development Policy, is characterised by a hilly-gullied region. Pursuing more available land from surrounding loess mountains and gullies has caused changes to the topography by way of excavation, backfill, transformation, and irrigation. These seriously destroy the fragile loess environment [11–14]. It is becoming widely accepted that strength degradation of loess, induced by damage to interparticle bonding resulting from strata erosion, could be deemed as the main cause of various scales of catastrophic slope sliding [15, 16] and instability in northwest China [17–37]. Nowadays, a significant body of research studies has indicated that the mechanical behavior of soil is related not only to its microstructural characteristics but also to its stress history and loading regime. Some other research studies discussed the interactions of landslide deposit with terrace sediment and mobility characteristics [38–42]. Mofiz and Islam [43] investigated the stress-strain and interfacial frictional behaviour of nonwoven geotextile reinforced residual soils and presented the simplified prediction procedures for determining the strength of reinforced and unreinforced soils under various stress paths. Many researchers have recognized that stress-path testing can be useful in exploring and investigating the failure mechanism of soil either through perspective of stress-strain relationship or through pore pressure behaviour [44]. Jiang et al. [45] studied the deformation characteristics of natural loess from Jingyang, about 13 km north of Xi'an, Shaanxi Province, China, under

the stress paths around a shield tunnel [46–53]. They concluded that in a complete unloading path, the natural loess behaves in a linear elastic manner, whereas in a complete loading path, the natural loess presents nonlinear and plastic behaviour. Macro-availability of silt in the vicinity of Delhi, India, has resulted in these alluvial deposits being named Delhi silt, and it consists primarily of silt (35–80%), varying amounts of sand (10–43%) with insignificant clay content (3–7%) [54]. Usmani et al. [54] evaluated the stress-strain-volume change and pore pressure behaviour of Delhi silt under the conventional triaxial compression (CTC) and reduced triaxial extension (RTE) test for four values of confining pressures (including 100, 150, 200, and 300 kPa) and concluded that Delhi silt is transitional and can be described by neither a sand nor a clay-type framework [55, 56]. The stress-strain-volume change, pore pressure behaviour, and shear strength were found to be affected by the amount of fines content present in the sand and the loading regime. Results obtained from the above research studies show that the mechanical behavior of soil is stress-path dependent.

Numerous researchers have sought an environment-friendly construction material towards achieving sustainable development. Lian et al. [57] have recognized that the control of strata erosion is a crucial problem, particularly in northwest China, and it can be achieved using loess reinforced by root. The effect of *Robinia pseudoacacia* root distribution patterns including horizontal, vertical, and crossed reinforcement on the shear strength was explored, and the crossed reinforced pattern was found to be most effective in the control of strata erosion. Zhang et al. [58] also studied the shear strength of plain soil specimens and composites consisted of roots of *Robinia pseudoacacia* and soil from the Chinese Loess Plateau and concluded that roots have more impacts on the cohesion of the loess than the friction angle. Other researchers improved the shearing behaviour of loess using the postharvest waste and revealed that the improvement of shear strength is attributed to the effect of interlocking, induced by the presence of post-harvest waste [2]. This outcome may be further interpreted using the PIV technology [59] and the triaxial-erosion apparatus [60]. These studies explore the potential for insertion of agricultural waste straw and plant root to improve the shearing behaviour of natural soils towards controlling strata erosion. However, studies exploring the stress-strain relationship, the pore pressure behaviour, and the critical state behaviour for the loess soils reinforced with agricultural waste straw under different stress paths are remarkably limited.

The objectives of this paper are as follows: (a) to investigate the stress-strain relation and the pore pressure behaviour of Lantian loess and reinforced Lantian loess under conventional triaxial compression (CTC) for three confining pressures, (b) to compare with other soils, namely, Jingyang loess and Delhi silt, reported in the literature under reduced triaxial compression (RTC) and reduced triaxial extension (RTE), respectively, with emphasis on strength uniqueness and critical state behaviour, to highlight the effect of the presence of agricultural waste straw, and (c) to explore the potential for the use of agricultural waste straw as a recycled reinforcement material to prevent instability of loess body as subjected to quick surface thick fills.

2. Materials and Methods

2.1. Sampling Location and Preparation of Specimens. A 1 m^3 block sample of natural loess from Lantian, about 22 km southeast of Xi'an, was used for preparing a series of remoulded cylinder specimens of 80 mm in height and 39.1 mm in diameter. A higher degree of saturation for the remoulded cylinder specimens was achieved by using a combination of vacuum saturation and backpressure saturation techniques. Details in relation to the preparation of the remoulded cylinder specimens are as follows:

(1) Place the natural material in an electric oven; dry the natural material using the temperature of 105° for 24 hours; measure the natural water content.

(2) Crush the dried natural material; treat the agricultural waste straw with boiled water.

(3) Pave material in disk; add a proper amount of water and %waste straw = 0.6 to the materials (a water content of 18% was considered in this work); place materials in a moist chamber for two days to ensure the uniformity of water content in soil.

(4) Compact the material in mould by three layers; the mass of materials for each layer can be calculated in accordance with the designated void ratio of 0.9.

(5) Extrude the cylinder specimen from mould.

(6) Saturate the remoulded cylinder specimen using a combination of vacuum saturation and backpressure saturation methods.

The physical properties for Lantian loess are summarised in Table 1. The particle-size distribution curves of Lantian loess are presented in Figure 1. The material was classed as low plasticity silt (ML) in accordance with the Unified Soil Classification System (USCS). The uniformity coefficient C_u varies from 9.26 to 15.26 although the majority of the material shares the same USCS symbol. The physical and mechanical properties for the agricultural waste straw are summarised in Table 2.

2.2. Stress-Path Testing. Conventional triaxial compression (CTC) tests were conducted using a VJ Tech triaxial apparatus for which the axial stress can reach a maximum of 2 MPa and the confining pressure that the triaxial cell is able to sustain can reach 1 MPa in maximum. The preparation of the remoulded specimens and the remoulded reinforced specimens was similar except for a preliminary process to soften the waste straw with boiling water (98°C). The saturation stage consisted of vacuum saturation for four to six hours and backpressure saturation for two to three days and was performed in accordance with the principle of pressure increments, under back pressure up to 120 kPa, to achieve a B value of about 0.98. All the pressure increments were imposed slowly, preventing restructuring of the specimens

Table 1: Physical properties of Lantian loess.

Sample ID	C_u	C_c	%clay	%silt	%sand	Unit weight γ_d (kN/m^3)	USCS symbol
S1a	9.26	1.94	10.0	83.4	6.6	13.72	ML
S1b	10.48	2.13	11.0	81.1	7.9	13.60	ML
S1c	15.26	2.79	10.0	84.0	6.0	13.83	ML

Note. USCS stands for the unified soil classification system; C_u is the coefficient of uniformity; C_c is the coefficient of gradation.

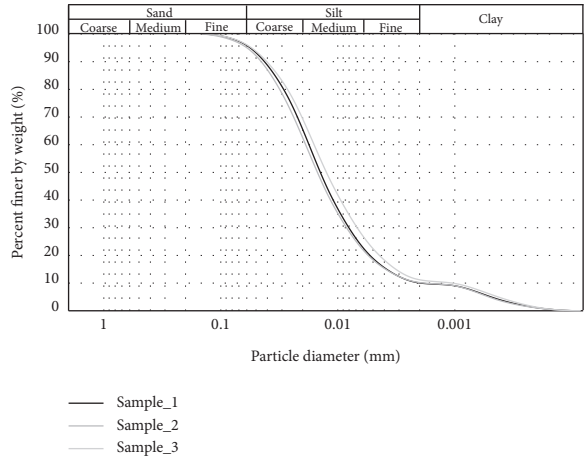

Figure 1: Particle-size distribution curves for Lantian loess.

Table 2: Physical and mechanical properties of agricultural waste straw.

Material	Diameter (mm)	Length (mm)	Unit weight (kN/m^3)	Tensile strength (MPa)	Elastic modulus (GPa)	Maximum tension (N)
Agricultural waste straw	3-4	10	2.3	135.8	5.9	52.8

from occurring. The saturation stage was immediately followed by the isotropic consolidation stage. The specimens were loaded along the isotropic compression path (path OA shown in Figure 2) at three values of confining pressures (including 200 kPa, 300 kPa, and 400 kPa) to backtrack their initial stress states. A degree of consolidation $U = 95\%$ was adopted as a discrimination criterion for terminating the consolidation stage. Undrained shearing of the remoulded specimens was performed at a rather slow rate of 0.05%/min, thereby allowing pore pressure changes to be equalised throughout the remoulded specimens.

Comparison with other two soils, namely, Jingyang loess and Delhi silt, reported in the literature [45, 54] under reduced triaxial compression (RTC) and reduced triaxial extension (RTE), respectively, with emphasis on strength uniqueness and critical state behaviour, was also made later in this paper to highlight the effect of the presence of waste straw. Stress-path testing details in relation to Jingyang loess and Delhi silt are given as follows. Jingyang loess, consisted of sand (12.1%), silt (83.1%), and clay (4.8%), was also dried using a manner as previously described and crushed for preparing a series of remoulded specimens of 80 mm in height and 39.1 mm in diameter in RTC tests. A B value of 0.98 indicated high degree of saturation, and the remoulded specimens were then consolidated at three confining

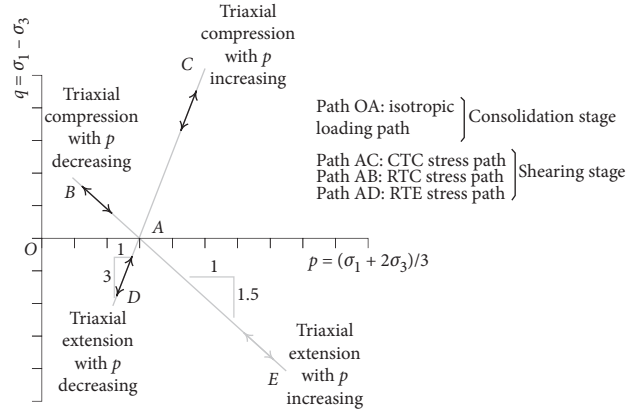

Figure 2: Three stress-path testings.

pressures of 50 kPa, 200 kPa, and 600 kPa, respectively. After the consolidation stage, undrained shearing was carried out. The loading rate of deviatoric stress q in the RTC test was determined using a ratio of the peak deviatoric stress of the CTC test $q_{\mathrm{CTC}}^{\mathrm{peak}}$ at the same confining pressure to the shear test time of the CTC test [45].

Delhi silt considered here generally comprises fine sand (20%), silt (73%), and clay (7%) [54]. The slurry-deposition

method [61] was used to produce remoulded specimens of homogeneous fabric and fairly uniform void ratio throughout. The preparation of the remoulded specimens was carried out in a Perspex tube mould with an inner diameter of 39 mm and height of 230 mm. Saturation was conducted under back pressure of up to 400 kPa and effective pressure of 10 kPa, leading to a B value of 0.98. The consolidation stage was completed in 30–40 days under a confining pressure of 100–125 kPa without reducing the back pressure levels, ensuring that the diffusion condition maintained during the saturation stage was not lost. Undrained shearing of the remoulded specimens was carried out very slowly with a strain rate of 0.2% (min). These shearing control measures were applied to the stress-path testings towards minimising the impacts of strain (or loading) rate on the strength characteristics of silt-clay soils [62].

3. Results

3.1. Conventional Triaxial Compression

3.1.1. Undrained Stress-Strain Behaviour. The consolidated undrained stress-strain relation of Lantian loess and reinforced Lantian loess confined at pressures of 200, 300, and 400 kPa under the CTC stress path is shown in Figure 3. q was found to increase with an increase in confining pressure, with a higher rate of increase observed for the reinforced Lantian loess. In the case of reinforced Lantian loess, q increased sharply at lower strains of up to 4%, and, thereafter, gradually as strain values moved towards 20%.

3.1.2. Pore Pressure Behaviour. The pore pressure response of Lantian loess and reinforced Lantian loess is shown in Figure 4(a). u for Lantian loess increased very quickly at lower strains for all confining pressures, and after reaching a peak value, a subtle fall in pore pressure was observed at higher strains. However, the reinforced Lantian loess showed a continuous increase in u for all the confining pressures. Relation of u/σ_3 versus axial strain ε_a for Lantian loess and reinforced Lantian loess is shown in Figure 4(b). From the results, it can be seen that u/σ_3 ratio reached a range of 0.34–0.24 at higher strains.

3.2. Reduced Triaxial Compression

3.2.1. Undrained Stress-Strain Behaviour. The undrained stress-strain relation of Jingyang loess under the RTC stress path for three confining pressures of 50, 200, and 600 kPa is shown in Figure 5. q was found to increase with increasing confining pressure. The higher the confining pressure, the higher the rate of increase in q. q went up very quickly at lower strain values of up to 1.5%, and after reaching peak values, a fall in q was observed at higher strains. Peak of q was attained irrespective of the confining pressures.

3.2.2. Pore Pressure Behaviour. The pore pressure response of Jingyang loess is shown in Figure 6. u decreased initially at lower strains for all the confining pressures, and after reaching a curve turning point, an increase in u was observed at higher strains, with a more pronounced effect at higher confining pressures, as shown in Figure 6(a). Relation of axial strain ε_a versus u/σ_3 for Jingyang loess is shown in Figure 6(b). At higher strains, u/σ_3 ratio reached 1.84 for the confining pressure = 50 kPa, reached 0.64 for the confining pressure = 200 kPa and reached 0.32 for the confining pressure = 600 kPa.

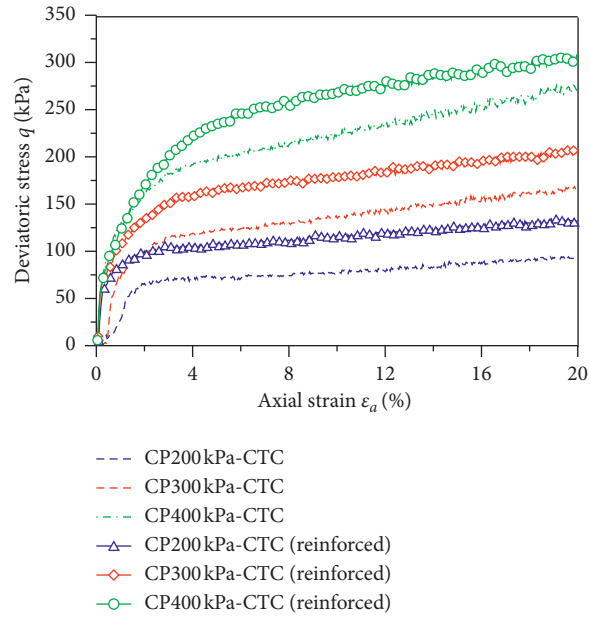

Figure 3: Undrained stress-strain relation of Lantian loess and reinforced Lantian loess under the CTC stress path.

3.3. Reduced Triaxial Extension

3.3.1. Undrained Stress-Strain Behaviour. The undrained strain-stress relation of Delhi silt under the RTE stress path for the four confining pressures of 100, 150, 200, and 300 kPa is shown in Figure 7. q increased with increase of confining pressure. The increase in q was found to be steeper for higher confining pressures. Peak of q was attained irrespective of the confining pressures. q increased very quickly at lower strains, and, thereafter, gradually until Delhi silt failed at strains around 10%.

3.3.2. Pore Pressure Behaviour. The pore pressure response of Delhi silt is shown in Figure 8. u rose significantly at lower strains, with a higher rate of increase observed at higher confining pressures, as shown in Figure 8(a). u at higher strains was found to be either constant or increasing with strain level. Relation of axial strain ε_a versus u/σ_3 for Delhi silt is shown in Figure 8(b). It can be seen from Figure 8(b) that at higher strains, u/σ_3 ratio varied ranging from −0.18 to −0.27.

4. Discussion

4.1. Stress-Strain Relation and Stress Path Character. The results shown in Figures 3, 5, and 7 indicate that the types of

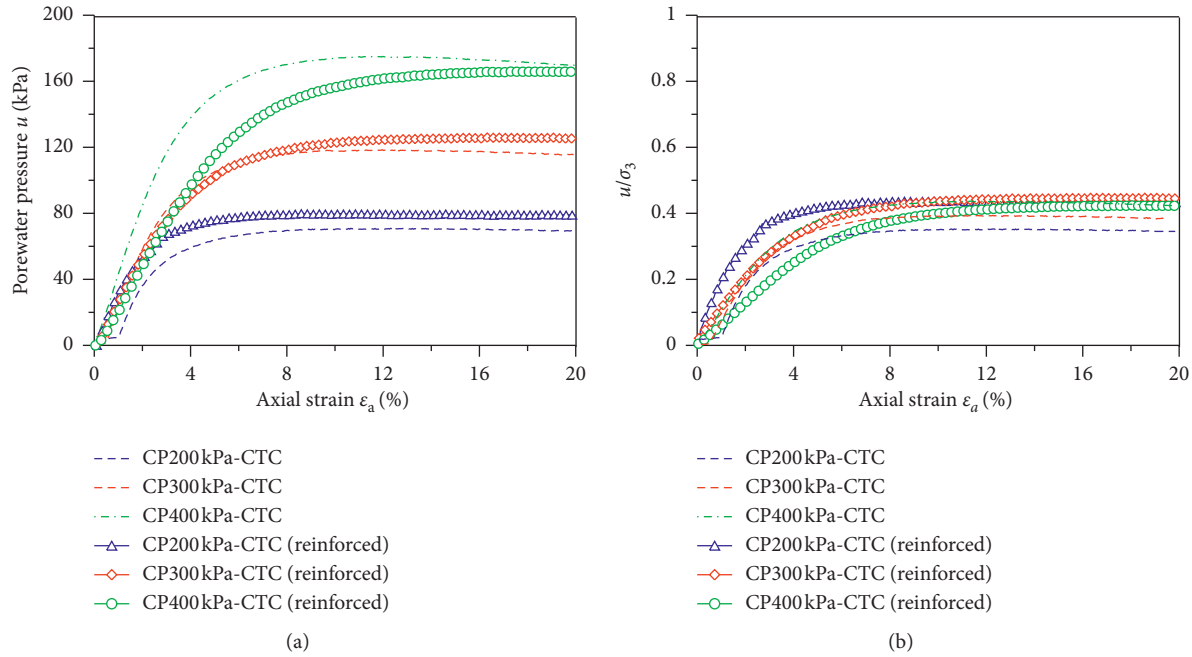

Figure 4: Pore pressure response of Lantian loess and reinforced Lantian loess under the CTC stress path: (a) pore pressure u versus axial strain ε_a and (b) u/σ_3 versus axial strain ε_a.

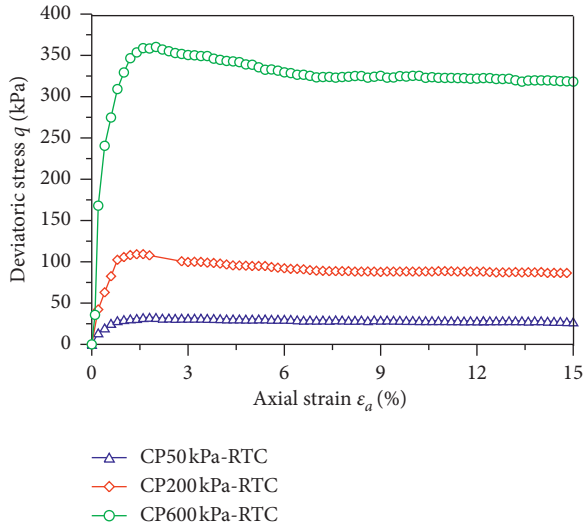

Figure 5: Undrained stress-strain relation of Jingyang loess under the RTC stress path.

stress-strain relations for the soils discussed here included strain-hardening and strain-softening. The stress-strain relation of Lantian loess and reinforced Lantian loess under the CTC stress path exhibited strain-hardening behaviour. The effective stress paths, using Cambridge stress parameters [63], for three confining pressures from consolidated undrained tests, are shown in Figure 9. The strain-hardening behaviour of Lantian loess was accompanied by the initial increase of effective mean stress p' and then the decrease of p' towards failure. The effective stress paths were observed not to end at the failure line but to travel along it as p' increased. The effective stress paths suggest that the loess was contractive in the first place, followed by a phase transformation and then dilative behaviour. The leading cause for Lantian loess to exhibit the significant dilative behaviour following the initial contraction was not attributed to its silt content and void ratio but to the difference in stress path. Its silt content deviates not much from that of the two other soils (Table 3). Also, Nocilla et al. [66] found that the stress-strain data for silt-clay soils with different specific volumes (or void ratio) at large strains are rather similar as the effect of confining pressure has been removed by normalisation using mean effective stress. There are no discernible trends with the specific volume, which is surprising as it might have been expected that the denser the specimen, the stiffer the behaviour. To support the made argument, comparisons with other silts worldwide were made to reveal the behind reason that addresses why there is a phase transformation here. Delhi silt and Jingyang loess exhibited contractive behaviour under RTE and RTC stress paths, respectively, and no phase transformation was observed, whereas Alaskan silt, Yazoo silt, LMVD silt, Italian silt, and Lantian loess, however, exhibited a phase transformation to dilative behaviour from contractive behaviour under CTC stress path (Table 3). From these results, it can be considered that the CTC stress path is likely to cause soils to be compacted dense enough to possess a high tendency to dilation when subjected to further stresses. The results conform with observations reported by various researchers [54, 64, 65].

The stress-strain relation of Jingyang loess under the RTC stress path behaved in a strain-softening manner. The effective stress paths for three confining pressures from consolidated undrained tests are also shown in Figure 9. Initially, the rate of increase of q was high and thereafter reduced as the shearing progressed towards the failure line.

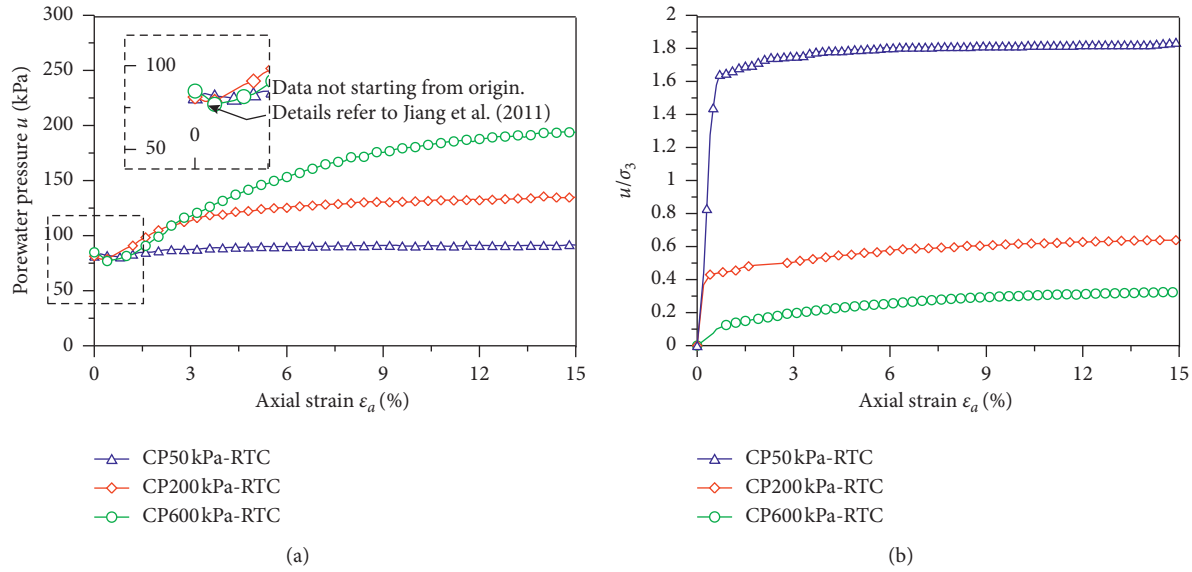

Figure 6: Pore pressure response of Jingyang loess under the RTC stress path: (a) pore pressure u versus axial strain ε_a and (b) u/σ_3 versus axial strain ε_a.

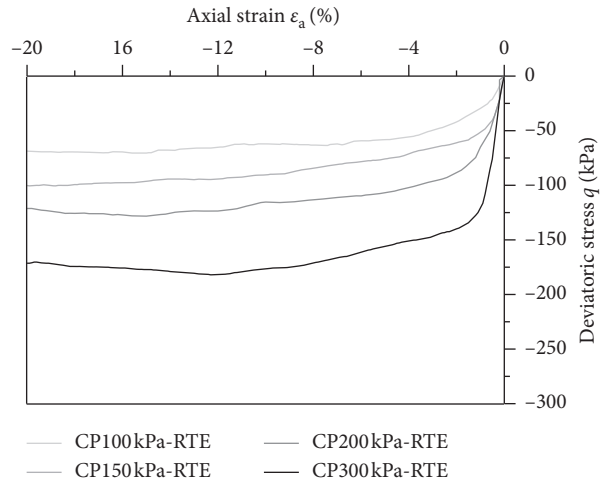

Figure 7: Undrained stress-strain relation of Delhi silt under the RTE stress path.

The effective stress paths ended at the failure line, and no movement along the failure line was observed. The nature of the effective stress paths indicates that Jingyang loess was contractive throughout, and no phase transformation and dilative behaviour were observed.

The stress-strain relation of Delhi silt under the RTE stress path was characterised by strain-softening. The effective stress paths for four confining pressures of 100, 150, 200, and 300 kPa from consolidated undrained tests are shown in Figure 10. It is noteworthy that the rate of increase of q was initially remarkably high and subsequently reduced when the shearing progressed towards failure of the specimen. No travel of the stress path along the failure line was observed. The effective stress paths suggest that Delhi silt was contractive throughout, indicating no phase transformation and dilative behaviour.

4.2. Comparison between Lantian Loess and Jingyang Loess and Delhi Silt on Stress-Strain Relation. As discussed, Lantian loess and reinforced Lantian loess exhibited strain-hardening behaviour in their stress-strain relations. In contrast, Jingyang loess and Delhi silt showed strain-softening behaviour. It can be considered that soils either under the RTC stress path or RTE stress path are likely to exhibit strain-softening behaviour, whereas soils under the CTC stress path are most difficult to exhibit strain-softening behaviour. Peak of q was attained at all confining pressures for Delhi silt under the RTE stress path as a result of localised deformation resulting from explicit necking formation in specimens. q seemed to have more pronounced effect at higher confining pressures (Figure 7).

Peak of q was attained at all confining pressures for Jingyang loess under the RTC stress path (Figure 5). This strain-softening behaviour was accompanied by the decrease in axial stress, induced by some difficulty in holding axial stress constant after the peak of q. It can also be seen that the pore pressure u was negative at the very beginning and then became positive, which deviates from common clay behaviour under RTC (Figure 6). For clays, u is positive firstly and then becomes negative with increase in axial strain. Furthermore, it is noteworthy that the peak of q seemed to appear later than the minimal u. These results could also be caused by the inability to appropriately manipulate the axial stress.

Apart from that, the anisotropy of consolidation could also be deemed as one of the greatest contributors. However, the anisotropy, during consolidation, can be more easily eliminated for remoulded specimens than that for undisturbed specimens because of interparticle bonds and fabric in undisturbed specimens. The anisotropy of consolidation, therefore, was neglected since all the specimens discussed here were not undisturbed specimens.

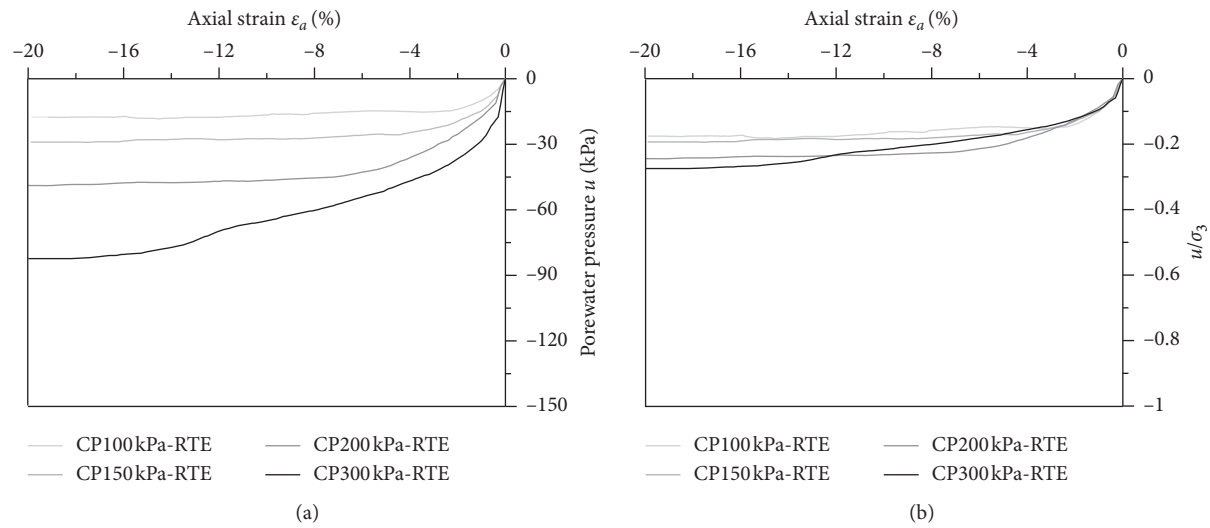

Figure 8: Pore pressure response of Delhi silt under the RTE stress path: (a) pore pressure u versus axial strain ε_a and (b) u/σ_3 versus axial strain ε_a.

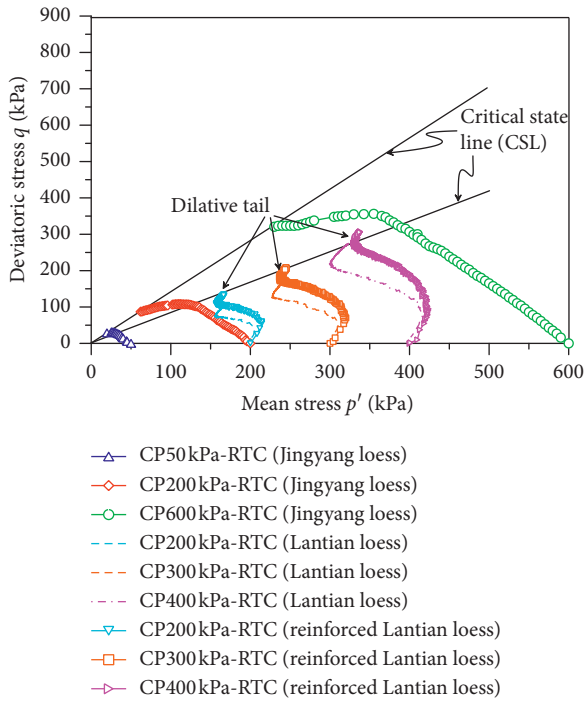

Figure 9: Effective stress paths of Lantian loess and Jingyang loess and failure line in $p' - q$ space.

4.3. Strength Envelopes. The strength envelopes from the results of undrained tests for Lantian loess, reinforced Lantian loess, Jingyang loess, and Delhi silt in compression and extension are shown in Figures 11 and 12, respectively. ϕ' for Lantian loess, reinforced Lantian loess, and Jingyang loess is 19.5°, 25.8°, and 34.3°, respectively, under compression loading conditions. ϕ' for Delhi silt is at a value of 36°–40° under extension loading conditions. The results show that ϕ' under RTE was largest and ϕ' under CTC was smallest. The results confirmed nonidentification of a unique failure line under different stress paths. Results of similar types of research on other silts are summarised in Table 3.

4.4. Critical State Behaviour. Figures 9 and 10 show the critical state line (CSL) of every soil in $p' - q$ space. The critical state line for Lantian loess and reinforced Lantian loess was not in line with that of Jingyang loess, indicating that the stress path did have implication on the critical state behaviour. As only one type of soil was sheared under extension loading conditions, the corresponding critical state was thus not analysed.

Wang et al. [64] and Nocilla et al. [66] indicated that the dilative tail on the stress path grows with decreasing clay content. From these results, it can be considered that Jingyang loess with %clay = 4.8 supposes to behave somewhat more like silt than Delhi silt with %clay = 7, which also corresponds to higher values of stiffness and undrained shear strength. This argument, however, contradicted the development of u under the same confining pressure for Jingyang loess and Delhi silt (Figures 6(a) and 8(a)) and the present strength values, namely, $\phi = 34.3°$ for Jingyang loess under RTC and $\phi = 36–40°$ for Delhi silt under RTE (Table 3). The main cause leading to this contradiction was the use of stress paths other than CTC stress path.

4.5. Enhanced Shear Strength Formation. The formation of enhanced shear strength for the reinforced Lantian loess is of great importance for researchers and practitioners widening the horizon of its application. Cheng et al. [67] indicated that insertion of the waste straw, during direct shearing of the loess-waste straw mixture, hampered particle dislocation because of the effect of interlocking towards impeding the development of shear bands in the vicinity of the shearing plane. From the deviatoric stress – axial strain relations (Figure 3), it can be seen that the tests were terminated at $\varepsilon_a = 20\%$ where the specimens were bulging appreciably. The

Table 3: Stress-strain-volume change and pore pressure comparison of remoulded silts under compression and extension tests.

Soil type	Particle-size distribution	Confining pressure	Stress-strain relation	Volumetric/pore pressure behaviour	Effective angle of friction ϕ'
Alaskan silt [64]	0–46% sand 49–57% silt 5–43% clay	NA	Strain-hardening in undrained shearing	Initial contraction, followed by dilative behaviour	32°–42° (CTC)
Yazoo silt and LMVD silt [65]	Yazoo silt: 3–18% sand, 70–82% silt, 13–16% clay LMVD silt: 8% sand, 80% silt, 12% clay	69–276 kPa	Strain-hardening in undrained shearing	Initial contraction, followed by dilative behaviour	28°–36° (CTC)
Italian silt [66]	5% sand 70% silt 25% clay	100–600 kPa	Strain-hardening in undrained shearing; strain-softening in drained shearing	Initial contraction, followed by dilative behaviour	NA
Delhi silt [54]	20% sand 73% silt 7% clay	100–300 kPa	Strain-softening in undrained shearing (peak stresses observed blow 20% strain level)	Contraction all long and no phase transformation observed	36°–40° (RTE)
Jingyang loess [45]	12.1% sand 83.1% silt 4.8% clay	50–600 kPa	Strain-softening in undrained shearing	Contraction all long and no phase transformation observed	34.3° (RTC)
Lantian loess (present study)	6–7.9% sand 81–84% silt 10–11% clay	200–400 kPa	Strain-hardening in undrained shearing	Initial contraction, followed by dilative behaviour	19.5° (CTC) 25.8° (CTC, reinforced)

Note. NA = not applicable.

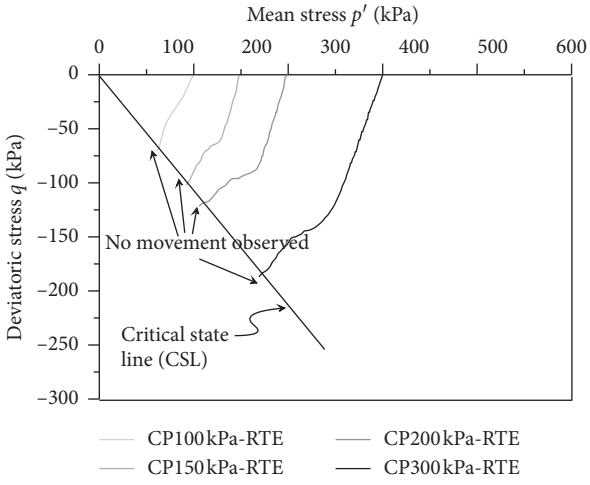

Figure 10: Effective stress paths of Delhi silt and failure line in $p' - q$ space.

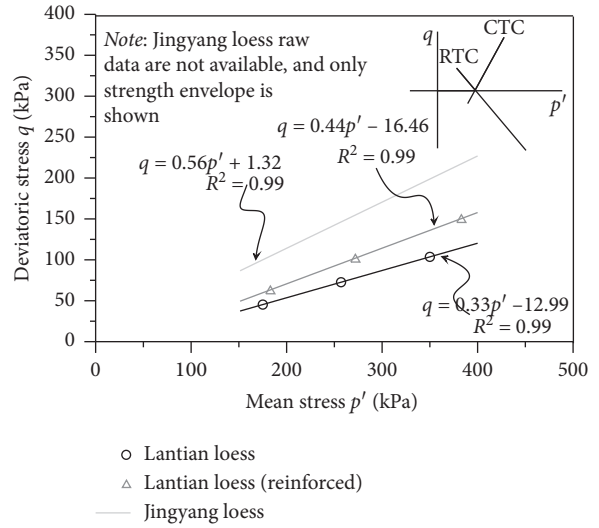

Figure 11: Strength envelopes of Lantian loess and reinforced Lantian loess as well as Jingyang loess in compression tests.

initial slopes for the reinforced Lantian loess were steeper than those for the unreinforced Lantian loess at all confining pressures, and the stiffness of the soils was increased with increasing the confining pressure. The pore pressure u also increased with increasing the confining pressure (Figure 4). It is well known that the u generated is attributed to the tendency of the soil to contract or dilate throughout the undrained shearing. The pore pressures were higher for the reinforced Lantian loess than the unreinforced Lantian loess. This higher u was generated because of the effect of waste straw on the development of volumetric deformation. Specifically, this higher u developed through distributing shear stresses within specimen by the waste straws towards increasing the tendency to develop contractive volumetric deformations within the mixture of soil fabric. The tendency to contract or dilate is indicated by the slope in the plot of u versus ε_a. A positive slope indicates contractive behaviour, and a negative slope suggests dilative behaviour. Since the slope after the peak, in turn, became negative from positive,

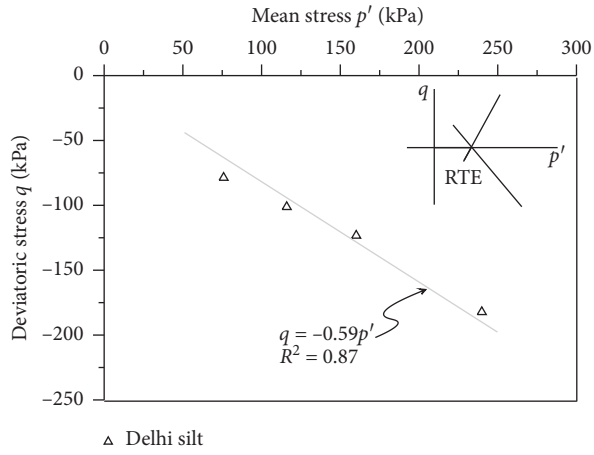

Figure 12: Strength envelope of Delhi silt in extension tests.

it can be concluded that the specimens contracted initially and then exhibited dilative behaviour when the waste straws were no longer able to restrain the dilation of the mixture. These results are in agreement with the findings of Peters et al. [68], Ahmad et al. [69], and Li [70].

4.6. Comparison of Present and Previous Studies. In order to verify the results observed in the present study, several relevant studies were compared in terms of the strength uniqueness and critical state behaviour. Jiang et al. [45] compared the critical state behaviour of natural loess, natural filling in ground fissure, and their corresponding remoulded soils under compression tests and found that the critical states in $p' - q$ space in compression tests almost lie on one line. Usmani et al. [54] conducted the stress-path testing on remoulded specimens of Delhi silt containing two proportions of silt and recognized the lack of identification of a unique critical state line under CTC and RTE stress paths. Yin and Chang [71] compared the critical state behaviour of various soft soils and found that the critical state line determined from undrained compression tests is not identical to that determined from undrained extension tests. Conventional elastic-plastic cap models can only predict a unique critical state line for the compression and extension tests. This may be deemed as the main cause to lead to misleading interferences about the nonuniqueness of critical state line. In summary, the previous studies provide strong support for the nonuniqueness of critical state line identified in the present study.

5. Conclusions

This study investigated the stress-strain relation and the pore pressure behaviour of Lantian loess and reinforced Lantian loess under the CTC stress path for three confining pressures. Comparison with Jingyang loess and Delhi silt who have essentially similar relative fraction of silt to clay, with emphasis on strength uniqueness and critical state behaviour, was conducted. Based on the results and discussion, some main conclusions can be drawn as follows:

(1) The Lantian loess and the reinforced Lantian loess under the CTC stress path behaved strain-hardening behaviour, while Jingyang loess and Delhi silt under the RTC and RTE stress paths, respectively, behaved strain-softening behaviour. Peak of q attained at all confining pressures for Delhi silt under RTE was because of the localised deformation caused by the explicit necking formation in tested specimens resulting in the strain-softening behaviour.

(2) ϕ' under RTE was largest, whereas ϕ' under CTC was smallest, hence confirming nonidentification of a unique failure line under different stress paths. Comparable results of similar types of research on other silts were found. On the other hand, the stress path did have implication on the critical state behaviour.

(3) The higher pore pressure, generated within the reinforced Lantian loess, developed through distributing shear stresses within specimen by the waste straws, thereby increasing the tendency to develop contractive volumetric deformations within the mixture of soil fabric. Since the loess has been deemed to be susceptible to seepage failure, this study explores the exciting potential for the use of agricultural waste straw as a recycled reinforcement material towards preventing instability of loess body in hilly-gullied regions of northwest China as subjected to quick surface thick fills. The findings are useful in controlling loess slope stability, and the proposed recycled reinforcement material has extensive application prospect.

Data Availability

The experimental data used to support the findings of this study are included within the article.

Conflicts of Interest

The authors declare that they have no conflicts of interest.

Authors' Contributions

This paper represents a result of collaborative teamwork. Miss Lin Wang and Mr. Zhong-Fei Xue performed a series of laboratory tests. Dr. Wen-Chieh Cheng guided laboratory tests and prepared the original manuscript. He also gave edits for the revised manuscript. The three authors contributed equally to this work.

Acknowledgments

This study would not have been possible without financial supports from the Special Fund for Basic Scientific Research of Central Colleges, Chang'an University, under grant no. 300102269502.

References

[1] W. C. Cheng, J. C. Ni, S. L. Shen, and Z. F. Wang, "Modeling of permeation and fracturing grouting in sand: laboratory investigations," *Journal of Testing and Evaluation*, vol. 46, no. 5, pp. 2067–2082, 2018.

[2] W.-C. Cheng, G. Li, N. Liu, J. Xu, and S. Horpibulsuk, "Recent massive incidents for subway construction in soft alluvial deposits of Taiwan: a review," *Tunnelling and Underground Space Technology*, vol. 96, Article ID 103178, 2019.

[3] A. Gonzalez-Ollauri and S. B. Mickovski, "Plant-soil reinforcement response under different soil hydrological regimes," *Geoderma*, vol. 285, pp. 141–150, 2017.

[4] G. Modoni, P. Croce, and L. Mongiovì, "Theoretical modelling of jet grouting," *Géotechnique*, vol. 56, no. 5, pp. 335–347, 2006.

[5] G. Modoni and J. Bzówka, "Analysis of foundations reinforced with jet grouting," *Journal of Geotechnical and Geoenvironmental Engineering*, vol. 138, no. 12, pp. 1442–1454, 2012.

[6] G. Modoni, A. Flora, S. Lirer, M. Ochmański, and P. Croce, "Design of jet grouted excavation bottom plugs," *Journal of Geotechnical and Geoenvironmental Engineering*, vol. 142, no. 7, Article ID 04016018, 2016.

[7] S.-L. Shen, Z.-F. Wang, S. Horpibulsuk, and Y.-H. Kim, "Jet grouting with a newly developed technology: the Twin-Jet method," *Engineering Geology*, vol. 152, no. 1, pp. 87–95, 2013a.

[8] S.-L. Shen, Z.-F. Wang, W.-J. Sun, L.-B. Wang, and S. Horpibulsuk, "A field trial of horizontal jet grouting using the composite-pipe method in the soft deposits of Shanghai," *Tunnelling and Underground Space Technology*, vol. 35, pp. 142–151, 2013b.

[9] X. Wang, M.-M. Hong, Z. Huang et al., "Biomechanical properties of plant root systems and their ability to stabilize slopes in geohazard-prone regions," *Soil and Tillage Research*, vol. 189, pp. 148–157, 2019a.

[10] W.-Y. Xia, Y.-J. Du, F.-S. Li et al., "In-situ solidification/stabilization of heavy metals contaminated site soil using a dry jet mixing method and new hydroxyapatite based binder," *Journal of Hazardous Materials*, vol. 369, pp. 353–361, 2019.

[11] Y. Leng, J. Peng, Q. Wang, Z. Meng, and W. Huang, "A fluidized landslide occurred in the Loess Plateau: a study on loess landslide in South Jingyang tableland," *Engineering Geology*, vol. 236, pp. 129–136, 2018.

[12] J. Peng, P. Ma, Q. Wang et al., "Interaction between landsliding materials and the underlying erodible bed in a loess flowslide," *Engineering Geology*, vol. 234, pp. 38–49, 2018.

[13] J. B. Peng, X. Tong, S. K. Wang, and P. H. Ma, "Three-dimensional geological structures and sliding factors and modes of loess landslides," *Environmental Earth Sciences*, vol. 77, p. 675, 2018.

[14] R. Xu, X. Li, W. Yang, C. Jiang, and M. Rabiei, "Use of local plants for ecological restoration and slope stability: a possible application in Yan'an, Loess Plateau, China," *Geomatics, Natural Hazards and Risk*, vol. 10, no. 1, pp. 2106–2128, 2019.

[15] U. Haque, P. F. da Silva, G. Devoli et al., "The human cost of global warming: deadly landslides and their triggers (1995–2014)," *Science of the Total Environment*, vol. 682, pp. 673–684, 2019.

[16] H. Shu, M. Hürlimann, R. Molowny-Horas et al., "Relation between land cover and landslide susceptibility in Val d'Aran, Pyrenees (Spain): historical aspects, present situation and forward prediction," *Science of the Total Environment*, vol. 693, Article ID 133557, 2019.

[17] Z. Duan, W.-C. Cheng, J.-B. Peng, Q.-Y. Wang, and W. Chen, "Investigation into the triggering mechanism of loess landslides in the south Jingyang platform, Shaanxi province," *Bulletin of Engineering Geology and the Environment*, vol. 78, no. 7, pp. 4919–4930, 2018.

[18] X. Fan, Q. Xu, G. Scaringi, S. Li, and D. Peng, "A chemo-mechanical insight into the failure mechanism of frequently occurred landslides in the Loess Plateau, Gansu Province, China," *Engineering Geology*, vol. 228, pp. 337–345, 2017.

[19] W.-Z. Guo, Z.-X. Chen, W.-L. Wang et al., "Telling a different story: the promote role of vegetation in the initiation of shallow landslides during rainfall on the Chinese Loess Plateau," *Geomorphology*, vol. 350, Article ID 106879, 2020.

[20] T.-F. Gu, M.-S. Zhang, J.-D. Wang, C.-X. Wang, Y.-J. Xu, and X. Wang, "The effect of irrigation on slope stability in the Heifangtai Platform, Gansu Province, China," *Engineering Geology*, vol. 248, pp. 346–356, 2019.

[21] X. Hou, S. K. Vanapalli, and T. Li, "Water infiltration characteristics in loess associated with irrigation activities and its influence on the slope stability in Heifangtai loess highland, China," *Engineering Geology*, vol. 234, pp. 27–37, 2018.

[22] Y. Li and P. Mo, "A unified landslide classification system for loess slopes: a critical review," *Geomorphology*, vol. 340, pp. 67–83, 2019.

[23] P. Li, W. Shen, X. Hou, and T. Li, "Numerical simulation of the propagation process of a rapid flow-like landslide considering bed entrainment: a case study," *Engineering Geology*, vol. 263, Article ID 105287, 2019.

[24] H. Luo, F. Wu, J. Chang, and J. Xu, "Microstructural constraints on geotechnical properties of Malan Loess: a case study from Zhaojiaan landslide in Shaanxi province, China," *Engineering Geology*, vol. 236, pp. 60–69, 2018.

[25] X. Pei, X. Zhang, B. Guo, G. Wang, and F. Zhang, "Experimental case study of seismically induced loess liquefaction and landslide," *Engineering Geology*, vol. 223, pp. 23–30, 2017.

[26] D. Peng, Q. Xu, X. Zhang et al., "Hydrological response of loess slopes with reference to widespread landslide events in the Heifangtai terrace, NW China," *Journal of Asian Earth Sciences*, vol. 171, pp. 259–276, 2019.

[27] J. Peng, Z. Fan, D. Wu et al., "Heavy rainfall triggered loess-mudstone landslide and subsequent debris flow in Tianshui, China," *Engineering Geology*, vol. 186, pp. 79–90, 2015.

[28] J. Peng, Z. Fan, D. Wu et al., "Landslides triggered by excavation in the loess plateau of China: a case study of Middle Pleistocene loess slopes," *Journal of Asian Earth Sciences*, vol. 171, pp. 246–258, 2019.

[29] J. S. Shi, L. Z. Wu, S. R. Wu, B. Li, T. Wang, and P. Xin, "Analysis of the causes of large-scale loess landslides in Baoji, China," *Geomorphology*, vol. 264, pp. 109–117, 2016.

[30] X. Wang, J. Wang, H. Zhan, P. Li, H. Qiu, and S. Hu, "Moisture content effect on the creep behavior of loess for the catastrophic Baqiao landslide," *Catena*, vol. 187, Article ID 104371, 2020.

[31] G. Wang, D. Zhang, G. Furuya, and J. Yang, "Pore-pressure generation and fluidization in a loess landslide triggered by the 1920 Haiyuan earthquake, China: a case study," *Engineering Geology*, vol. 174, pp. 36–45, 2014.

[32] S. Wang, J. Peng, J. Zhuang, C. Kang, and Z. Jia, "Underlying mechanisms of the geohazards of macro Loess discontinuities on the Chinese Loess Plateau," *Engineering Geology*, vol. 263, Article ID 105357, 2019b.

[33] L. Xu, F. C. Dai, L. G. Tham, Y. F. Zhou, and C. X. Wu, "Investigating landslide-related cracks along the edge of two loess platforms in northwest China," *Earth Surface Processes and Landforms*, vol. 37, no. 10, pp. 1023–1033, 2012.

[34] L. Xu, F. C. Dai, X. B. Tu et al., "Occurrence of landsliding on slopes where flowsliding had previously occurred: an investigation in a loess platform, North-west China," *Catena*, vol. 104, pp. 195–209, 2013.

[35] L. Xu, M. R. Coop, M. Zhang, and G. Wang, "The mechanics of a saturated silty loess and implications for landslides," *Engineering Geology*, vol. 236, pp. 29–42, 2018.

[36] F. Y. Zhang and G. H. Wang, "Effect of irrigation-induced densification on the post-failure behavior of loess flowslides occurring on the Heifangtai area, Gansu, China," *Engineering Geology*, vol. 236, pp. 111–118, 2017.

[37] S. Zhang, X. Pei, S. Wang, R. Huang, X. Zhang, and Z. Chang, "Centrifuge model testing of a loess landslide induced by rising groundwater in Northwest China," *Engineering Geology*, vol. 259, Article ID 105170, 2019.

[38] G. B. Crosta, S. Imposimato, and D. Roddeman, "Numerical modelling of entrainment/deposition in rock and debris-avalanches," *Engineering Geology*, vol. 109, no. 1-2, pp. 135–145, 2008.

[39] G. B. Crosta, S. Imposimato, D. Roddeman, and P. Frattini, "On controls of flowike landslide evolution by anerodible layer," in Landslide Science and Practice, C. Margottini et al., Ed., Springer, Berlin, Heidelberg, pp. 263–270, 2013.

[40] O. Hungr, "A model for the runout analysis of rapid flow slides, debris flows, and avalanches," *Canadian Geotechnical Journal*, vol. 32, no. 4, pp. 610–623, 1995.

[41] O. Hungr, "Rock avalanche occurrence, process and modelling," *Landslides*, vol. 302, pp. 243–266, 2006.

[42] A. Mangeney, O. Roche, O. Hungr, N. Mangold, G. Faccanoni, and A. Lucas, "Erosion and mobility in granular collapse over sloping beds," *Journal of Geophysical Research Earth Surface*, vol. 115, pp. 3–40, 2010.

[43] S. A. Mofiz and M. N. Islam, "Assess the stress-train and interfacial frictional behavior of nonwoven geotextile reinforced residue soils." GeoFlorida 2010," in *Advances in Analysis, Modeling & Design, Geotechnical Special Publication No. 199*, D. O. Fratta, A. J. Puppala, and B. Muhunthan, Eds., American Society of Civil Engineers, Orlando, FL, USA, pp. 823–832, 2010.

[44] L. R. Hoyos, D. D. Pérez-Ruiz, and A. J. Puppala, "Refined true triaxial apparatus for testing unsaturated soils under suction-controlled stress paths," *International Journal of Geomechanics*, vol. 12, no. 3, pp. 281–291, 2012.

[45] M. Jiang, H. Hu, J. Peng, and S. Leroueil, "Experimental study of two saturated natural soils and their saturated remoulded soils under three consolidated undrained stress paths," *Frontiers of Architecture and Civil Engineering in China*, vol. 5, no. 2, pp. 225–238, 2011.

[46] W.-C. Cheng, J. C. Ni, A. Arulrajah, and H.-W. Huang, "A simple approach for characterising tunnel bore conditions based upon pipe-jacking data," *Tunnelling and Underground Space Technology*, vol. 71, pp. 494–504, 2018.

[47] W.-C. Cheng, J. C. Ni, H.-W. Huang, and J. S. Shen, "The use of tunnelling parameters and spoil characteristics to assess soil types: a case study from alluvial deposits at a pipejacking project site," *Bulletin of Engineering Geology and the Environment*, vol. 78, no. 4, pp. 2933–2942, 2019.

[48] W. Wei, Z. Shao, Y. Zhang, R. Qiao, and J. Gao, "Fundamentals and applications of microwave energy in rock and concrete processing—a review," *Applied Thermal Engineering*, vol. 157, Article ID 113751, 2019.

[49] Y. Zhang, Z. Shao, W. Wei, and R. Qiao, "PFC simulation of crack evolution and energy conversion during basalt failure process," *Journal of Geophysics and Engineering*, vol. 16, no. 3, pp. 639–651, 2019.

[50] J. L. Qiu, H. Q. Liu, J. X. Lai, H. P. Lai, J. X. Chen, and K. Wang, "Investigating the long-term settlement of a tunnel built over improved loessial foundation soil using jet grouting technique," *Journal of Performance of Constructed Facilities*, vol. 32, no. 5, Article ID 04018066, 2018.

[51] J. L. Qiu, Y. W. Qin, J. X. Lai et al., "Structural response of the metro tunnel under local dynamic water environment in loess strata," *Geofluids*, vol. 2019, Article ID 8541959, 16 pages, 2019.

[52] J. X. Lai, X. L. Wang, J. L. Qiu, J. X. Chen, Z. N. Hu, and H. Wang, "Extreme deformation characteristics and countermeasures for a tunnel in difficult grounds in southern Shaanxi, China," *Environmental Earth Sciences*, vol. 77, no. 19, p. 706, 2018.

[53] W.-C. Cheng, L. Wang, Z.-F. Xue, J. C. Ni, M. Rahman, and A. Arulrajah, "Lubrication performance of pipejacking in alluvial deposits," *Tunnelling and Underground Space Technology*, vol. 91, Article ID 102991, 2019.

[54] A. Usmani, G. V. Ramana, and K. G. Sharma, "Experimental evaluation of shear-strength behavior of Delhi silt under static loading conditions," *Journal of Materials in Civil Engineering*, vol. 23, no. 5, pp. 533–541, 2011.

[55] P. Anantanasakul, J. A. Yamamuro, and V. N. Kaliakin, "Stress-strain and strength characteristics of silt-clay transition soils," *Journal of Geotechnical and Geoenvironmental Engineering*, vol. 138, no. 10, pp. 1257–1265, 2012.

[56] S. Shapiro and J. A. Yamamuro, "Effects of silt on three-dimensional stress-strain behavior of loose sand," *Journal of Geotechnical and Geoenvironmental Engineering*, vol. 129, no. 1, pp. 1–11, 2003.

[57] B. Lian, J. Peng, H. Zhan, and X. Wang, "Mechanical response of root-reinforced loess with various water contents," *Soil and Tillage Research*, vol. 193, pp. 85–94, 2019.

[58] C.-B. Zhang, L.-H. Chen, Y.-P. Liu, X.-D. Ji, and X.-P. Liu, "Triaxial compression test of soil-root composites to evaluate influence of roots on soil shear strength," *Ecological Engineering*, vol. 36, no. 1, pp. 19–26, 2010.

[59] M. I. Peerun, D. E. L. Ong, and C. S. Choo, "Interpretation of geomaterial behavior during shearing aided by PIV technology," *Journal of Materials in Civil Engineering*, vol. 31, no. 9, Article ID 04019195, 2019.

[60] A. Mehdizadeh, M. M. Disfani, R. Evans, and A. Arulrajah, "Progressive internal erosion in a gap-graded internally unstable soil: mechanical and geometrical effects," *International Journal of Geomechanics*, vol. 18, no. 3, Article ID 04017160, 2018.

[61] R. Kuerbis and Y. P. Vaid, "Sand sample preparation-the slurry deposition method," *Soils and Foundations*, vol. 28, no. 4, pp. 107–118, 1988.

[62] R. Nikhilesh and S. Parth, "Strain rate behavior of compacted silt," *Journal of the Geotechnical Engineering Division*, vol. 102, no. 4, pp. 347–360, 1976.

[63] K. H. Roscoe, A. N. Schofield, and C. P. Wroth, "On the yielding of soils," *Géotechnique*, vol. 8, no. 1, pp. 22–53, 1958.

[64] J. L. Wang, V. Vivatrat, and J. R. Rusher, "Geotechnical properties of Alaska OCS silts," in *Proceedings of the 14th Annual Offshore Technology Conference (OTC 4412)*, pp. 415–420, Houston, TX, USA, 1982.

[65] T. L. Brandon, A. T. Rose, and J. M. Duncan, "Drained and undrained strength interpretation for low-plasticity silts," *Journal of Geotechnical and Geoenvironmental Engineering*, vol. 132, no. 2, pp. 250–257, 2006.

[66] A. Nocilla, M. R. Coop, and F. Colleselli, "The mechanics of an Italian silt: an example of 'transitional' behaviour," *Géotechnique*, vol. 56, no. 4, pp. 261–271, 2006.

[67] W.-C. Cheng, Z.-F. Xue, L. Wang, and J. Xu, "Using post-harvest waste to improve shearing behaviour of loess and its validation by multiscale direct shear tests," *Applied Sciences*, vol. 9, no. 23, p. 5206, 2019.

[68] J. F. Peters, E. S. Berney, and I. V. Bovney, "Percolation threshold of sand-clay binary mixtures," *Journal of Geotechnical and Geoenvironmental Engineering*, vol. 136, no. 2, pp. 310–318, 2010.

[69] F. Ahmad, F. Bateni, and M. Azmi, "Performance evaluation of silty sand reinforced with fibres," *Geotextiles and Geomembranes*, vol. 28, no. 1, pp. 93–99, 2010.

[70] C. Li, *Mechanical response of fiber-reinforced soil*, Ph.D. Dissertation, The University of Texas at Austin, Austin, TX, USA, 2005.

[71] Z.-Y. Yin and C. S. Chang, "Non-uniqueness of critical state line in compression and extension conditions," *International Journal for Numerical and Analytical Methods in Geomechanics*, vol. 33, no. 10, pp. 1315–1338, 2009.